

Heavy Ion Physics Prospects with the ATLAS Detector at the LHC

N. Grau, for the ATLAS Collaboration

Columbia University, Nevis Laboratories
Irvington, NY, USA, 10533

E-mail: ncgrau@nevis.columbia.edu

Abstract. The next great energy frontier in Relativistic Heavy Ion Collisions is quickly approaching with the completion of the Large Hadron Collider and the ATLAS experiment is poised to make important contributions in understanding QCD matter at extreme conditions. While designed for high- p_T measurements in high-energy $p + p$ collisions, the detector is well suited to study many aspects of heavy ion collisions from bulk phenomena to high- p_T and heavy flavor physics. With its large and finely segmented electromagnetic and hadronic calorimeters, the ATLAS detector excels in measurements of photons and jets, observables of great interest at the LHC. In this talk, we highlight the performance of the ATLAS detector for Pb+Pb collisions at the LHC with special emphasis on a key feature of the ATLAS physics program: jet and direct photon measurements.

PACS numbers: 25.75.Bh, 25.75.Cj

Submitted to: *J. Phys. G: Nucl. Phys.*

1. Introduction

The advent of an era where two relativistic heavy ion physics colliders are running simultaneously at the LHC and at RHIC is upon us. The RHIC program has moved from its initial discovery phase into making detailed measurements to further understand the strongly-interacting quark-gluon plasma formed in $Au + Au$ collisions. The LHC heavy ion program provides an opportunity to perform complementary measurements at higher collision energy and to study the plasma with a different temperature and lifetime. Together RHIC and the LHC will be a focused, two-pronged attack on understanding QCD matter in extreme conditions.

The RHIC program has brought new insights on aspects of the entire collision evolution from the initial state parton distribution functions of the nuclei, through thermalization of the fireball, and the subsequent hadronization of the medium. Questions about the role of saturation physics came to light with the first measurements of charged particle multiplicity[1]. The large value of the measured elliptic flow, v_2 , for

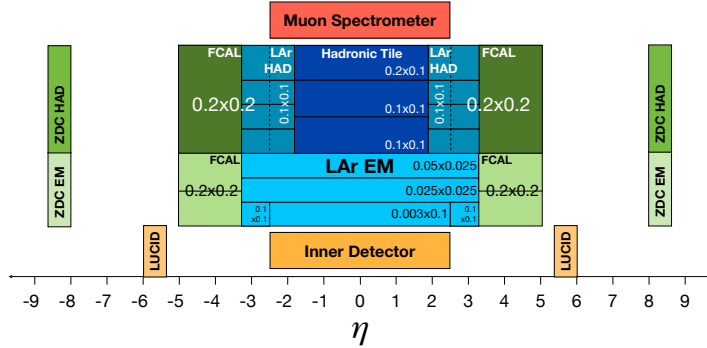


Figure 1. The η view of the different subdetectors of the ATLAS, all subdetectors cover the full 2π in azimuth. Tracking and muon detection extends to $|\eta| < 2.5$. Both the electromagnetic and hadronic calorimeters cover $|\eta| < 5$ and are longitudinally segmented with the typical $\Delta\eta \times \Delta\phi$ segmentation indicated.

all particles up to and including heavy flavor mesons together with hydrodynamical calculations indicate that the matter produced is strongly interacting with a low shear viscosity-to-entropy density ratio, a perfect fluid, instead of a dilute gas of partons[2]. J/ψ suppression was observed at RHIC. But the quantitatively similar suppression of SPS and RHIC data suggests that additional physics, such as recombination, which enhance the J/ψ signal at RHIC is required[3]. Jet quenching was discovered as a suppression of high- p_T hadrons[4] and confirmed by the away-side suppression from two-particle azimuthal correlations[5]. Novel structures, such as the “shoulder”[6] and the “ridge”[7] have been measured in heavy ion collisions. Even with this large amount of data on jet energy loss and its effect on the medium, the exact nature of energy loss is poorly understood. Single particle measurements (R_{AA}) are apparently insensitive to details of energy loss[8] as are two-particle correlations, being predominantly due to punch-through and tangential emission[9, 10].

Measurements at the LHC should elucidate these issues that are currently not well understood at RHIC. “Day-1” measurements such as the charged particle multiplicity will provide key constraints to saturation physics. Measurements of the collective flow of particles are crucial to determine if a perfect fluid state exists at the LHC. Quarkonia measurements, both bottomonium and charmonium, will give more detailed insight on the effects contributing to quarkonium suppression. Full jet reconstruction will reduce biases from energy loss, since the energy should be radiated predominantly close to the jet direction[11] and be reconstructed with the jet energy. The ATLAS prospects of global physics measurements[12] and quarkonia[13] capabilities are detailed elsewhere in these proceedings. The focus of this contribution is on measurements of jets and photons, those that will utilize the strengths of the ATLAS detector, in order to understand the details of energy loss of hard scattered partons in the medium.

2. Heavy Ion Physics Prospects

The ATLAS detector[14] is poised to make important contributions to the LHC heavy ion program in the coming $Pb+Pb$ runs. Although designed for high- p_T measurements of $p+p$ collisions at 14 TeV, the detector has been shown to be well suited to perform heavy ion measurements even at the extreme edge of currently predicted particle multiplicities ($dN/d\eta \sim 3000$)[15]. The ATLAS detector consists of inner tracking chambers followed by electromagnetic then hadronic calorimetry and finally a muon spectrometer. The ATLAS detector covers the full 2π in azimuth and Fig. 1 shows the η acceptance.

The unique feature of the ATLAS detector is its calorimetry. It is both electromagnetic and hadronic and covers 10 units of η , unprecedented coverage for relativistic heavy ion experiments. The notable feature of the calorimeter is its longitudinal segmentation with varying $\Delta\eta \times \Delta\phi$ segment sizes indicated in Fig. 1. Of particular importance is the first longitudinal electromagnetic segment. It is composed of strips in η with a typical width of 0.003 units in η and extends to $|\eta| \lesssim 2.5$ units. It was designed to measure $H \rightarrow \gamma\gamma$ events and to reject di-jet events. The importance of this layer for photon measurements is discussed in Section 2.2.

2.1. Jet Physics in ATLAS

Jet performance in heavy ion events has been studied for two complementary jet reconstruction algorithms, the seeded cone algorithm and the Fast- k_T algorithm[16]. These algorithms perform jet reconstruction on $0.1 \times 0.1 \Delta\eta \times \Delta\phi$ towers built from energy sums of the electromagnetic and hadronic calorimeters. For the seeded cone algorithm, the segment- and η -dependent $\langle E_T \rangle$ is subtracted prior to jet reconstruction. For the Fast- k_T algorithm jet reconstruction is performed directly on the full energy calorimeter towers. A set of discriminant variables is used to distinguish real jets from background jets composed of underlying event energy. After discrimination, the background jets are used to determine the background energy to be subtracted from the real jets.

The performance for jet reconstruction is evaluated by embedding entire PYTHIA di-jet events into unquenched HIJING events. All reconstructed jets were compared to the truth jets defined as jets reconstructed from the final state, generated particles.

The jet reconstruction efficiency and energy resolution for jets reconstructed in central, $dN/d\eta = 2700$, events with the cone and k_T algorithm are shown in upper panels of Fig. 2. Efficiency and resolution differences are observed for the lower E_T jets. The jet reconstruction has been studied as a function of HIJING inclusive charged-particle multiplicity for $|\eta| < 0.5$. The lower panels of Fig. 2 show the energy resolution of reconstructed cone jets as a function of E_T and η . The energy resolution improves with decreasing multiplicity and with η up to the region of the forward calorimeter (at $|\eta| > 3.2$) where the resolution becomes similar to that measured at midrapidity.

The reconstructed and fake cone jet spectra for $dN/d\eta = 2700$ is shown in the left panel of Fig. 3 and compared to the input PYTHIA jet spectrum. The raw reconstructed spectrum is uncorrected for efficiency and energy resolution. Still, the raw spectrum

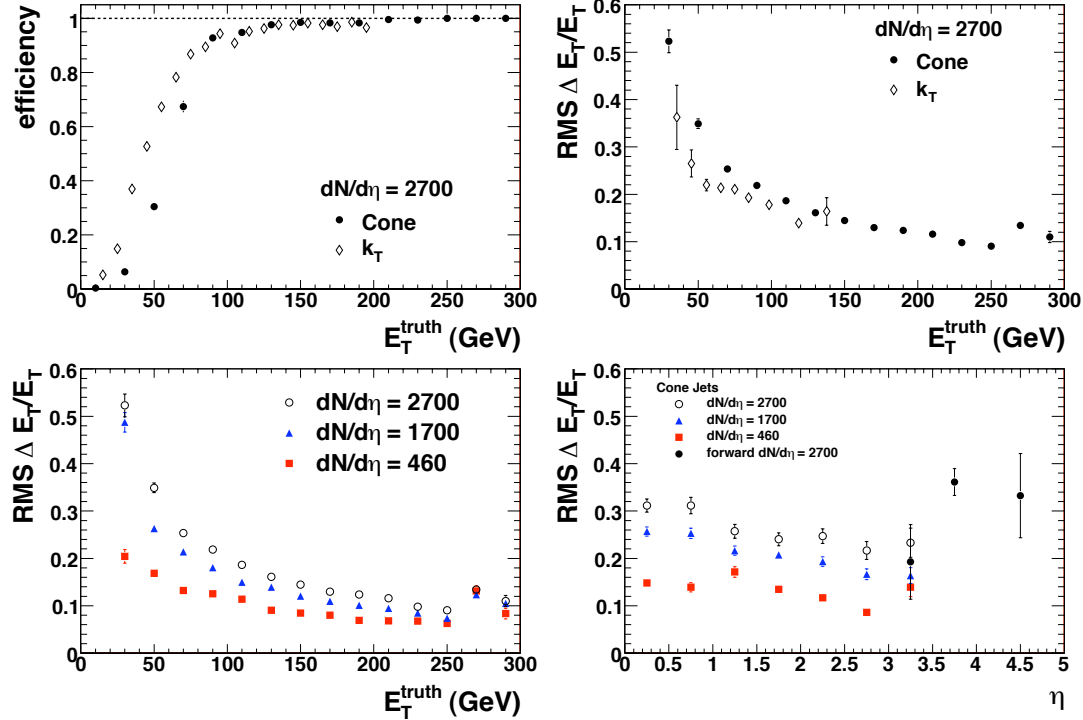


Figure 2. *Upper:* Comparison of the jet reconstruction efficiency (left) and jet energy resolution (right) for cone (filled) and k_T (open) algorithms from PYTHIA di-jet events embedded in unquenched HIJING. *Lower:* Energy resolution of cone jets as a function of E_T (left) and as a function of η (right) (for $E_T > 70$ GeV) for several HIJING $dN/d\eta$. The filled circles indicate a forward, $|\eta| > 3$, sample of embedded jets.

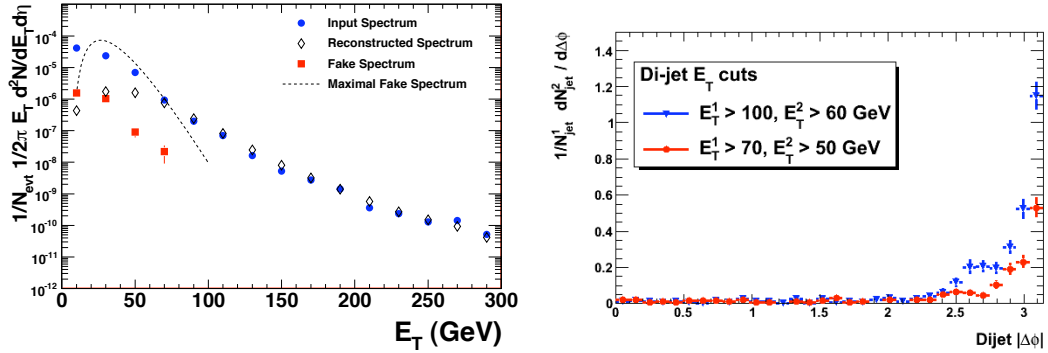


Figure 3. *Left:* Inclusive jet spectra: input PYTHIA (filled circles), raw reconstructed (open diamonds), raw fake jets (dashed line), and fake jets after rejection (squares) for cone jets reconstructed from PYTHIA di-jet events embedded in HIJING $dN/d\eta = 2700$. The raw spectrum is uncorrected for efficiency and energy resolution. *Right:* The $\Delta\phi$ distribution between reconstructed cone jets in two different jet energy ranges.

matches the input distribution well for $E_T > 80$ GeV. The maximal fake rate was evaluated from unquenched HIJING events. Rejection of fake jets was performed by making a cut on the shape of the energy distribution within the jet. A fake fraction of

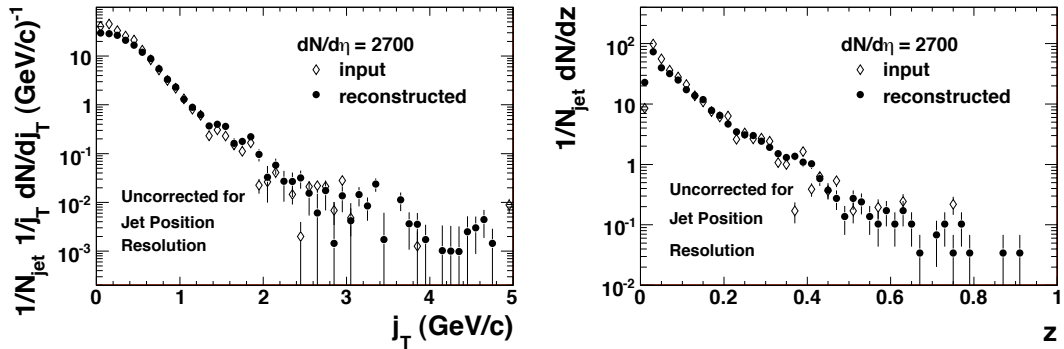


Figure 4. The j_T distribution (left) and the fragmentation function (right) from raw reconstructed (closed) and input PYTHIA distribution (open) for $E_T > 70$ GeV jets. The raw distributions have not been corrected for jet position resolution.

less than a few percent is achieved with minimal loss of efficiency for jets above 50 GeV.

ATLAS will also perform di-jet studies. The $\Delta\phi$ distribution between reconstructed cone jets is shown in the right panel of Fig. 3 for two different E_T cuts for the jet pairs. The distribution is plotted as a conditional probability of observing the second, lower- E_T jet given the trigger, higher- E_T jet. This distribution has not been corrected for efficiency or energy and position resolution. Still, integration of the higher jet E_T data yields a 60% probability of observing a jet above 60 GeV given a jet above 100 GeV in the event. Such a high probability before corrections reflects the high efficiency and large acceptance for jets in the ATLAS calorimeter.

New and varied measurements more sensitive to energy loss will be available for study with fully reconstructed jets. Two examples are measurements of the fragmentation function, $D(z) = 1/N_{\text{jet}} dN/dz$, and the j_T distribution. For jets, z is the longitudinal momentum fraction of a fragment with respect to the jet and j_T is the transverse momentum of a fragment with respect to the jet. Both distributions are predicted to be sensitive to details of the energy loss[11, 17]. Jet fragments are measured from charged tracks in the inner detector[12], extrapolated to the calorimeter, and matched to the reconstructed jet. These distributions of charged fragments from PYTHIA jets embedded in unquenched HIJING events are shown in Fig. 4. The open points are the PYTHIA distributions and the closed points are the reconstructed distributions. The latter are corrected for the tracking efficiency and any difference between the truth and reconstructed distributions are due to jet position resolution.

2.2. Direct Photons in ATLAS

The measurement of direct photons is another important tool for understanding the mechanism of energy loss. Direct photons can be used as a means to pin down the Q^2 of the initial hard scattering process to study the medium modification of the single, recoil jet. Unfortunately, direct photons are amongst a large background of photons from hadronic decays. An NLO pQCD calculation[18] predicts a direct photon signal

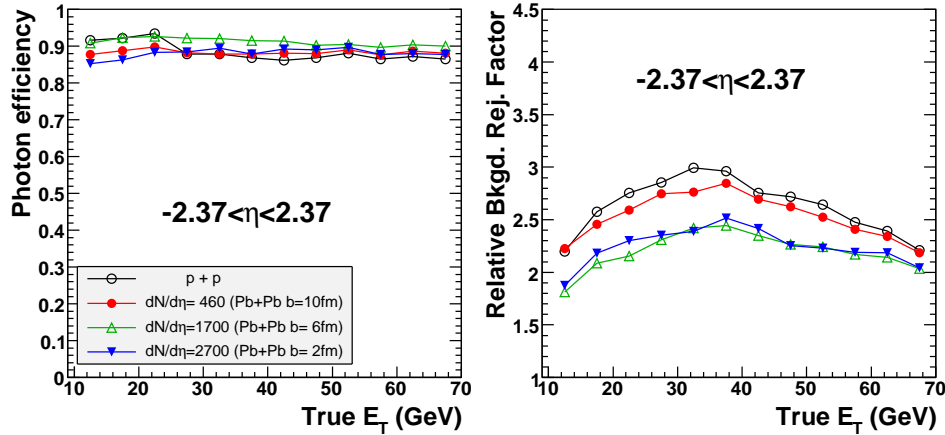


Figure 5. Photon identification efficiency (left) and relative rejection (right) for photon-identification cuts from the strip layer of the calorimeter. The cuts are tuned to give 90% efficiency.

to decay photon background of 2-10% from 30-100 GeV photons at $\sqrt{s} = 5.52$ TeV. To measure direct photons, reconstructed electromagnetic clusters are subjected to shower shape cuts and to isolation criteria to suppress the substantial background from hadronic decays.

The ATLAS calorimeter was uniquely designed specifically to perform such isolation and shape analysis for photons by rejecting di-jets for the purpose of Higgs searches, *i.e.* $H \rightarrow \gamma\gamma$. The $\Delta\eta$ segmentation of the front longitudinal electromagnetic (strip) layer is typically about 0.003 units. With this segmentation photons from π^0 decays can be separated over a wide range of E_T . Also, because of the fine segmentation, the occupancy is quite small. In unquenched HIJING events with $dN/d\eta = 2700$, the background contributes only a few hundred MeV to a cell whereas a few GeV photon will contribute typically half of its energy to the cell in the strip layer. Therefore, the efficiency of making identification cuts based on the information from the strip layer is only weakly dependent on centrality (see Fig. 5).

A series of shape variables can be constructed based on the energy distribution in the strip layer. These cuts have been tuned separately for each of the different HIJING multiplicity samples that have been simulated. The resulting efficiency and rejection of these tuned cuts for several multiplicities is shown in Fig. 5. This particular set of cuts is “loose” so as to keep the efficiency high at $\sim 90\%$ with a resulting relative rejection of up to 3. A set of “tight” cuts has also been tuned which results in 50% efficiency with rejection up to a factor of 6. Though these rejections are not enough to overcome the large background from hadronic decays, it should be sufficient to perform a statistical subtraction and extract the spectrum of non-decay photons within jets, which come from photon fragmentation and may be enhanced by jet-medium bremsstrahlung photons[19].

Isolation criteria based on calorimetric energy and track p_T within various cone sizes centered on the photon have been explored to gain additional rejection. These isolation

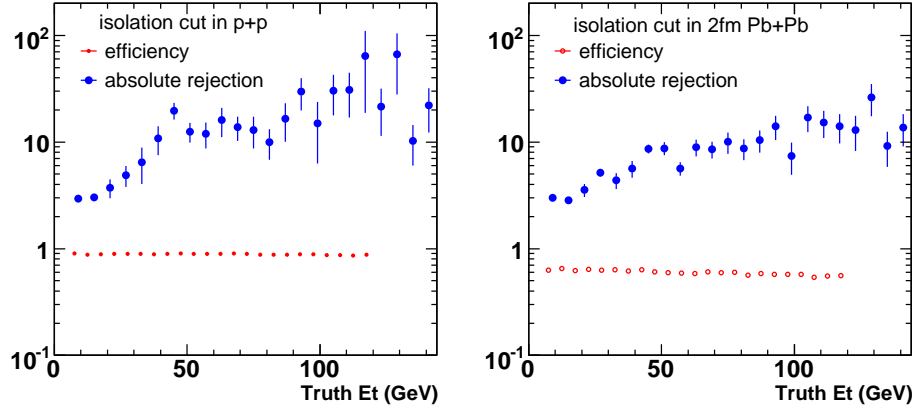


Figure 6. The efficiency (open) and the absolute rejection (filled) of the isolation criteria on direct photon measurements in $p + p$ (left) and $Pb + Pb$ collisions with $dN/d\eta = 2700$ (right).

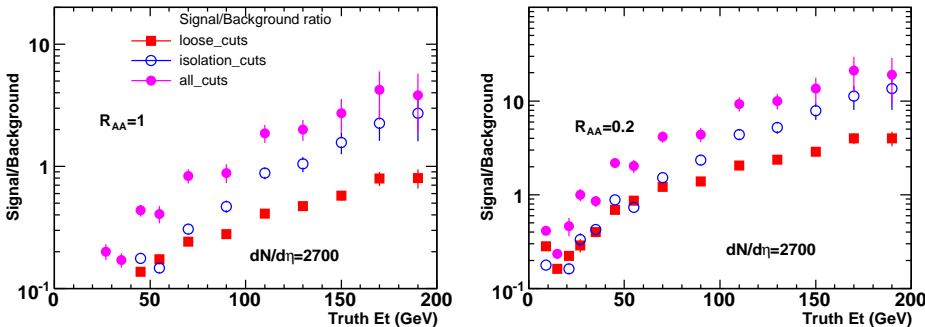


Figure 7. Photon signal to hadronic decay background ratio for unsuppressed hadrons (left) and for suppressed hadrons (right). The ratio is shown for the shape cuts (squares), isolation cuts (open circles), and combined (closed circles).

criteria are a strong function of centrality and have been tuned for different multiplicities by requiring the highest rejection with at least 50% efficiency. For example, for $dN/d\eta = 2700$, the isolation requirement within a cone of $R=0.2$ is $\sum E_T < 31$ GeV and no reconstructed track with $p_T > 2.5$ GeV. The rejection and efficiency of these cuts as a function of photon E_T are shown in Fig. 6.

Combining the shape cuts with the isolation results in substantial background rejection. The resulting direct photon signal to hadronic decay background is shown in Fig. 7. The ratio, with unsuppressed hadrons ($R_{AA} = 1$), is ~ 1 at 70 GeV increasing rapidly with E_T . However, if a factor of 5 suppression of hadrons from energy loss is measured at the LHC ($R_{AA} = 0.2$), the ratio is ~ 1 at 30 GeV. Assuming 0.5 nb^{-1} of data per LHC year and a reconstruction efficiency of 50%, 2×10^5 direct photons are expected with $E_T > 30$ GeV where the signal-to-background ratio is $\gtrsim 1$.

3. Conclusions

A full set of measurements are being planned to carry out the ATLAS heavy ion physics program. Jets, photons, global observables[12], quarkonia[13] and other heavy flavor physics are being explored. The uniquely designed calorimeter will make jet and photon measurements a key strength of the ATLAS heavy ion program. The large acceptance and longitudinal segmentation results in high efficiency, more than 70% for $E_T > 70$ GeV, and high energy resolution, better than 25% for $E_T > 70$ GeV, at the highest expected multiplicities. Direct photons will be measured with good efficiency, above 50%, and large signal-to-background, S/B more than 1 for $E_T > 30$ GeV, because of the uniquely designed strip layer of the electromagnetic calorimeter. With these measurements ATLAS is capable of making key measurements which will elucidate the nature of energy loss in the QCD medium.

4. Note

The figures shown here were based on studies using modified versions of ATLAS production software. Thus, they should be considered “ATLAS preliminary”. For completeness, version 12.0.6 of Athena software was used for generation, simulation, embedding, and reconstruction augmented only by the jet background subtraction software discussed.

Reference

- [1] Back B *et al.* [PHOBOS Collaboration] 2000 *Phys. Rev. Lett.* **85** 3100
- [2] Arsene I *et al.* [BRAHMS Collaboration] 2005 *Nucl. Phys.* **A757** 1
Back B B *et al.* [PHOBOS Collaboration] 2005 *Nucl. Phys.* **A757** 28
Adams J *et al.* [STAR Collaboration] 2005 *Nucl. Phys.* **A757** 102
Adcox K *et al.* [PHENIX Collaboration] 2005 *Nucl. Phys.* **A757** 184
- [3] Adare A *et al.* [PHENIX Collaboration] 2007 *Phys. Rev. Lett.* **98** 232301
- [4] Adcox K *et al.* [PHENIX Collaboration] 2002 *Phys. Rev. Lett.* **88** 022301
- [5] Adler C *et al.* [STAR Collaboration] 2003 *Phys. Rev. Lett.* **90** 083202
- [6] Adler S S *et al.* [PHENIX Collaboration] 2006 *Phys. Rev. Lett.* **97** 052301
- [7] Putschke J *et al.* [STAR Collaboration] 2006 *AIP Conf. Proc.* **842** 119
- [8] Renk T 2006 *Preprint* arXiv:hep-ph/0608333
- [9] Renk T 2006 *Phys. Rev.* **C74** 024903
- [10] Dainese A, Loizides C, and Paic G 2005 *Eur. Phys. J.* **C38** 461
- [11] Salgado C A and Wiedemann U A 2004 *Phys. Rev. Lett.* **93** 042301
- [12] Steinberg P *these proceedings*
- [13] Lebedev A *these proceedings*
- [14] *ATLAS Technical Design Report Volume 1*, CERN-LHCC-99-14
ATLAS Technical Design Report Volume 2, CERN-LHCC-99-15
- [15] *ATLAS Heavy Ion Physics Letter of Intent*, CERN-LHCC-2004-009
- [16] Cacciari M and Salam G P 2006 *Phys. Lett.* **B641** 57
- [17] Armesto N, Cunqueiro L, Salgado C A and Xiang W C 2008 *JHEP* **0802** 048
- [18] Aversa F, Chiappetta P, Greco M, and Guillet J P 1989 *Nucl. Phys.* **B327** 105
- [19] Turbide S, Gale C, Jeon S, and Moore G D 2005 *Phys. Rev.* **C72** 014906